Nanoparticle-induced twist-grain boundary phase

Maja Trček,[1] George Cordoyiannis,[1, 2, *] Vassilios Tzitzios,[3] Samo
Kralj,[4] George Nounesis,[3] Ioannis Lelidis,[2] and Zdravko Kutnjak[1, 5]

[1] *Condensed Matter Physics Department, Jožef Stefan Institute, 1000 Ljubljana, Slovenia*
[2] *Department of Physics, National and Kapodistrian University of Athens, 15784 Zografou, Greece*
[3] *Biomolecular Physics Laboratory, National Centre for Scientific Research "Demokritos", 15310 Aghia Paraskevi, Greece*
[4] *Faculty of Natural Sciences and Mathematics, University of Maribor, 2000 Maribor, Slovenia*
[5] *Jožef Stefan International Postgraduate School, 1000 Ljubljana, Slovenia*
(Dated: August 19, 2013)

By means of high-resolution ac calorimetry and polarizing optical microscopy it is demonstrated that surface-functionalized spherical CdSSe nanoparticles induce a twist-grain boundary phase when dispersed in a chiral liquid crystal. These nanoparticles can effectively stabilize the one-dimensional lattice of screw dislocations, thus establishing the twist-grain boundary order between the cholesteric and the smectic-A phases. A theoretical model is also presented accounting for the trapping of nanoparticles in the defect cores.

PACS numbers: 61.30.Jf,61.30.Mp,64.70.M-

I. INTRODUCTION

The existence of twist-grain boundary phases (TGBs) was theoretically predicted as the liquid-crystalline analogue of the Shubnikov phase exhibiting Abrikosov flux vortices in type-II superconductors [1, 2]. An isomorphism was proposed between liquid crystals and superconductors as follows: chiral nematic phase (N^*) - normal metal, twisted chiral line liquid (N_L^*) - Abrikosov vortex liquid, twist-grain boundary A (TGB_A) - Abrikosov vortex lattice, smectic-A (SmA) - Meissner phase [3]. TGBs were experimentally discovered by Goodby *et al.* [4] and Nguyen *et al.* [5], and later found in pure liquid crystals (LCs) or mixtures of LCs and chiral dopants [3, 6]. Their thermal signatures [7], X-ray patterns [8, 9], nuclear magnetic resonance spectra [10, 11] and optical textures [12] have been clearly identified. TGB_A phase consists of a one-dimensional lattice of screw dislocations along the grain boundaries that separate slabs of smectic order. This defect lattice is pinned for TGB_A, whereas it strongly oscillates in the case of N_L^* phase [13].

Various types nanoparticles have been often dispersed in liquid crystals in order to study the effects or quenched-random disorder on phase transitions [14–18], explore memory effects [19], tailor the dielectric and optical properties [20–22] and stabilize blue phases [23–25]. Very recently, it has been reported that surface-functionalized nanoparticles (NPs) that were initially used for blue phase stabilization [26], can also induce the TGB_A and N_L^* phases in a chiral liquid crystal [27]. This is so far shown only for one system composed of the chiral liquid crystal CE6 and surface-functionalized CdSe nanoparticles of a 3.5 nm diameter. It is not yet clear if such an effect, i.e., the nanoparticle-induced TGB order, is system-dependent or it exhibits a more general character. In this work we explore if the TGB_A and N_L^* phases can be induced in a different system of LC + NPs. The re-

sults are obtained by means of high-resolution ac calorimetry and polarizing optical microscopy, searching for the typical thermal and optical patterns of TGB order. In addition, the distinction of TGB_A and N_L^* optical textures has been ventured. The experimental results are accompanied by a brief theoretical model that accounts for the trapping of NPs in the one-dimensional lattice of screw dislocations.

II. SAMPLES AND EXPERIMENTAL METHODS

A high-purity chiral liquid crystal 4'-octyl-biphenyl-4-carboxylic acid 4-(2-methyl-butyl)-phenyl ester (CE8) was purchased from Merck and it was used without any additional treatment. The CdSSe NPs have been synthesized in N.C.S.R. "Demokritos". Atomic force microscopy measurements yield a diameter value of 3.4 ± 0.3 nm as shown in Fig. 1. The surface of NPs is treated with flexible chains of oleyl amine and tri octyl phosphine. Such a coating has been proven very effective for a good quality dispersion of various types of spherical or anisotropic NPs in liquid crystal hosts [24, 26–28].

One mixture with CdSSe concentration of $\chi = 0.05$ was prepared, where χ is defined as the mass of NPs over the total mass of the sample, i.e., $\chi = m_{NP}/(m_{LC} + m_{NP})$. For the mixture preparation a well-established protocol used in previous studies [24, 29] has been followed. This protocol includes the use of an ultrasonic bath to break any aggregates in the NPS solution, persistent mixing by magnetic stirring at elevated temperatures and, finally, pumping under vacuum in order to remove any solvent remains. Then the sample was placed in high-purity silver cells for calorimetric measurements and between glass plates for microscopic observations. Prior to measurements it was heated at temperatures corresponding to the isotropic phase of pure CE8.

The temperature profiles of heat capacity for pure CE8 and its mixture with CdSSe nanoparticles have been obtained using a fully-computerized, high-resolution ac calorimeter at Jožef Stefan Institute. This apparatus operates in the conventional ac as well as in relaxation (or non-adiabatic scanning) mode. The ac mode is mostly sensitive to continuous enthalpy

---

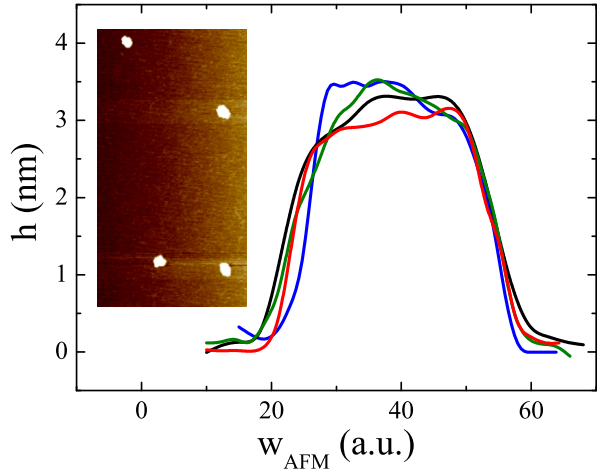*Corresponding author: george.cordoyiannis@ijs.si

FIG. 1: Atomic force microscopy measurements yield a diameter of 3.4 ± 0.3 nm for the CdSSe NPs.

changes, whereas the phase of the ac temperature oscillations indicates whether a transition is first or second order. The relaxation mode on the other hand is sensitive to both continuous and discontinuous (latent heat) enthalpy changes. The comparison of the data between the two modes of operation can provide a quantitative determination of the released latent heat. A detailed description of the apparatus is given in Ref. [30]. The heat capacity of the empty cell was subtracted in order to obtain the net specific heat capacity (C_p) of the samples.

The $\chi = 0.05$ mixture was additionally observed under a Carl Zeiss Jena microscope. The sample was placed between glass plates separated by 20 μm spacers. These plates are coated with a unidirectionally rubbed polyimide, thus, imposing planar anchoring conditions to the LC molecules. The images were captured under crossed polarizers. The temperature was stabilized and slowly changed by means of a home-made heating stage, with precision of ± 10 mK.

III. EXPERIMENTAL RESULTS AND DISCUSSION

Pure CE8 exhibits a single and sharp peak at 406.4 K associated with a direct, weakly first order N-SmA phase transition [24]. Contrary to pure CE8, the $\chi = 0.05$ mixture exhibits a completely different thermal behavior. Firstly, as shown by the cooling run with a rate of 0.25 Kh^{-1} in Fig. 2, the heat capacity anomaly is smeared and broadened due to the presence of CdSSe NPs. Secondly, the low temperature wing of the C_p anomaly reveals an additional smeared thermal signature, suggesting the presence of additional phase(s) between the N^* and the SmA ones. In order to more accurately probe the shape of this additional peak, a subsequent heating run was performed using a significantly slower scanning rate of 0.15 Kh^{-1}. This heating run revealed the presence of two small but clearly distinct anomalies corresponding to the typical pattern of a SmA-TGB$_A$-N_L^*-N^* phase sequence [7]. Note that
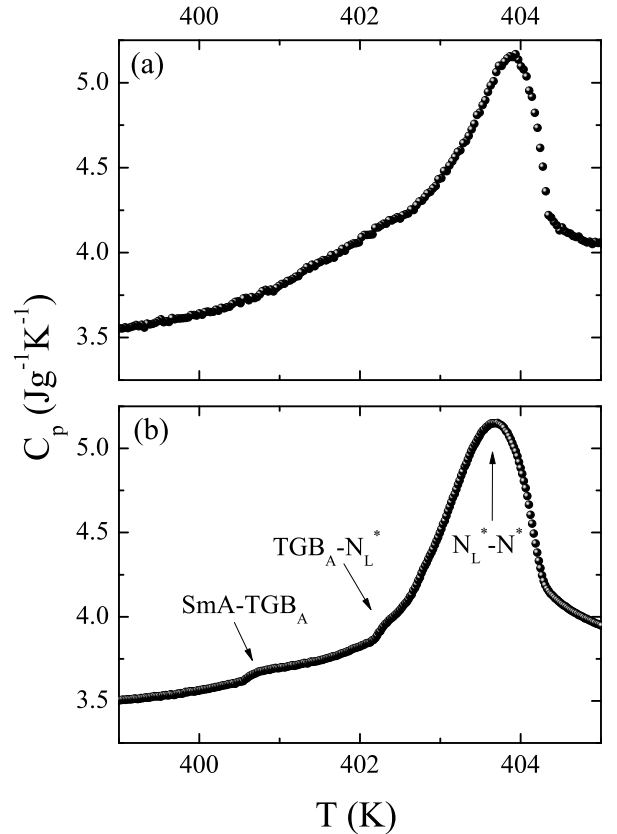

FIG. 2: The $C_p(T)$ profiles for the $\chi = 0.05$ mixture, upon cooling (a) with a rate of 0.25 Kh^{-1} and heating (b) of 0.15 Kh^{-1}. In both cases the low-temperature wing shows additional features that are more clearly visualized upon the (slower) heating. These features correspond to the characteristic thermal pattern SmA-TGB$_A$-N_L^*-N^* phase sequence [7, 27].

for systems composed of LC + NPs these additional anomalies, attributed to the SmA-TGB$_A$ and TGB$_A$-N_L^* phase transitions, appear more smeared [27] compared to the ones observed in pure liquid crystals [7].

Searching for additional experimental proof about the presence of the TGB$_A$ and N_L^* phases, the $\chi = 0.05$ mixture was observed under the microscope upon slow heating and cooling. Apart from the well-oriented SmA domains and the oily streaks characteristic of the N^* phase, two intermediate textures have been identified and they could be attributed to the TGB$_A$ and N_L^* structures. These textures can be seen in Fig. 3 for heating and in Fig. 4 for cooling. In case of heating, for TGB$_A$ the texture is similar with the one of SmA phase, although it becomes more colorful due to the continuous rotation of the smectic slabs. In addition, the elongated SmA fans are progressively attaining rounded edges. The fans become essentially wider and attain stripes along the next appearing N_L^* phase and finally change to the oily streaks in the N^* phase. Similar to the heating run, the subsequent cooling run reproduced nicely these four different textures corresponding to the aforementioned phases. To our knowledge, no other
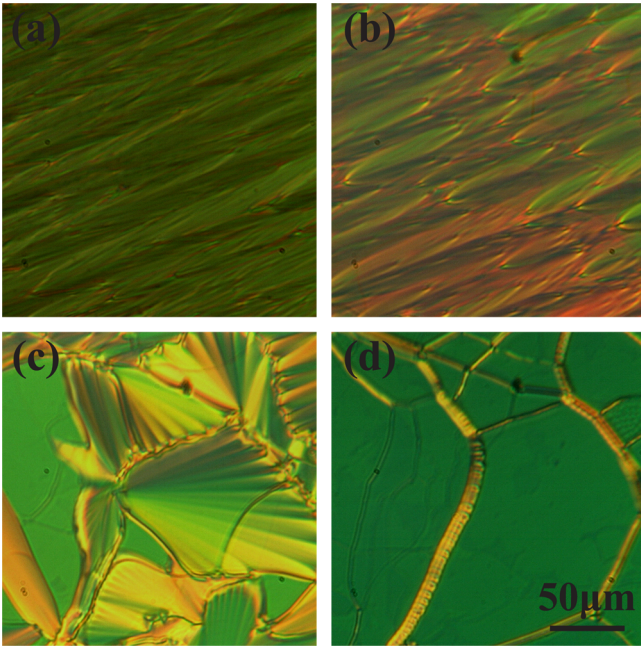
FIG. 3: Polarizing optical microscopy textures upon heating the $\chi = 0.05$ sample from the SmA phase; (a) SmA, (b) TGB$_A$, (c) N_L^* and (d) N^*. The images have been obtained under crossed polarizers.

FIG. 4: Polarizing optical microscopy textures upon cooling the $\chi = 0.05$ sample from the N^* phase; (a) N^*, (b) N_L^*, (c) TGB$_A$ and (d) SmA phase. The images have been obtained under crossed polarizers.

study has so far distinguished between the optical textures of TGB$_A$ and N_L^* structures.

The results obtained by both high-resolution calorimetry and microscopy demonstrate that the dispersion of CdSSe NPs induce TGB order in a narrow temperature range between the N^* and SmA phases. The effect has been briefly described by means of an adaptive-defect-core-targeting (ADCT) mechanism [27] for the system CE6 + CdSe NPs. In the following section the NP-induced stabilization of TGB order is discussed. Here the possible contribution of saddle-splay elasticity has been taken into account, something that was not yet considered in Ref. [27].

IV. THEORY

A simple Landau-de Gennes-Ginzburg mesoscopic appoach has been used in order to estimate the conditions under which NPs stabilize LC structures exhibiting a lattice of screw dislocations. The average volume fraction of NPs is given by

$$p = (N_{NP}v_{NP})/V_u \sim \chi(\rho_{LC}/\rho_{NPs}). \quad (1)$$

Here N_{NP} counts the number of NPs within a volume V_u, v_{NP} is the volume of a nanoparticle, χ measures the mass concentration of NPs, ρ_{NP} and ρ_{LC} stand for the mass densities of NPs and LC, respectively.

The local orientational ordering is determined by the headless nematic director field $\overrightarrow{n}$ and the translational ordering by the complex order parameter $\psi = \eta e^{i\phi}$. The amplitude η determines the degree of smectic ordering and the phase factor
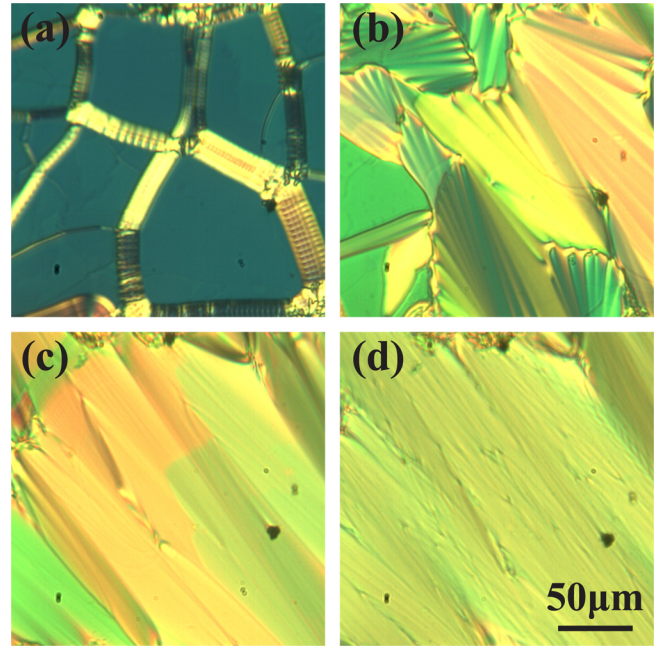
ϕ reveals the position of smectic layers. The orientational ordering within the Cartesian coordinate frame defined by the unit vector triad $\{\overrightarrow{e}_x, \overrightarrow{e}_y, \overrightarrow{e}_z\}$ is parametrized by

$$\overrightarrow{n} = \sin\theta_\parallel \sin\theta_\perp \overrightarrow{e}_x + \sin\theta_\parallel \cos\theta_\perp \overrightarrow{e}_y + \cos\theta_\parallel \overrightarrow{e}_z. \quad (2)$$

A. Free energy

The free energy density of the system is expressed as $f = f_c^{(s)} + f_e^{(n)} + f_e^{(s)}$. Here $f_c^{(s)}$ stands for the smectic condensation contribution, and $f_e^{(s)}$ and $f_e^{(n)}$ describe the smectic and nematic elastic penalties, respectively. In these terms only the most essential contributions are included in order to estimate the observed phase transition behavior.

The nematic elastic free energy penalty is expressed as [31]

$$\begin{aligned} f_e^{(n)} &= \frac{K_1}{2}(\nabla.\overrightarrow{n})^2 + \frac{K_2}{2}(\overrightarrow{n}.(\nabla \times \overrightarrow{n}) - q_{ch})^2 \\ &+ \frac{K_3}{2}|\overrightarrow{n} \times \nabla \times \overrightarrow{n}|^2 \\ &- \frac{K_{24}}{2}\nabla.(\overrightarrow{n}(\nabla.\overrightarrow{n}) + \overrightarrow{n} \times \nabla \times \overrightarrow{n}), \end{aligned} \quad (3)$$

where q_{ch} stands for the chirality-enforced wave vector, and K_1, K_2, K_3 and K_{24} determine the splay, twist, bend and saddle-splay Frank nematic elastic constant, respectively.

The smectic condensation and elastic free energy contributions are approximated by [31, 32]

$$f_c^{(s)} = \alpha_0 t |\psi|^2 + \frac{\beta}{2} |\psi|^4, \qquad (4)$$

$$f_e^{(s)} = C_\| |(\overrightarrow{n}.\nabla - iq_0)\psi|^2 + C_\perp |(\overrightarrow{n} \times \nabla)\psi|^2. \quad (5)$$

The quantities α_0, β are the positive Landau expansion coefficients, $t = (T - T_*)/T_*$ is the reduced dimensionless temperature, $C_\|$ and $C_\perp$ stand for the smectic compressibility and bend elastic constant, respectively. These constants are positive in the SmA phase and enforce one-dimensional SmA layering with a thickness of $d = 2\pi/q_0$, where the layer normal points along $\overrightarrow{n}$. For such a layer arrangement and $t < 0$ the condensation term enforces a degree of translational ordering given by

$$\eta_s = \sqrt{-t\alpha_0/\beta} \equiv \eta_0\sqrt{-t}. \qquad (6)$$

The corresponding smectic free energy condensation term reads

$$f_c^{(s)} = -\alpha_0 |t| \eta_s^2/2 = -\alpha_0 |t|^2 \eta_0^2/2. \qquad (7)$$

For the sake of simplicity we henceforth neglect the LC elastic anisotropy and set $C \equiv C_\| \sim C_\perp$ and $K \equiv K_1 \sim K_2 \sim K_3 \sim K_{24}$. The most important material-imposed lengths are the cholesteric pitch wavelength $P = 2\pi/q_{ch}$, the equilibrium smectic layer spacing $d = 2\pi/q_0$, the smectic order parameter correlation length ξ and the nematic twist penetration length λ. Below T_* the values of ξ and λ are estimated by

$$\xi = \sqrt{\frac{C}{\alpha_0 |t|}} \equiv \frac{\xi_0}{\sqrt{|t|}}, \qquad (8)$$

$$\lambda = \sqrt{\frac{K}{q_0^2 C \eta_s^2}} \equiv \frac{\lambda_0}{\sqrt{|t|}}. \qquad (9)$$

B. Geometry of the problem

The conditions under which TGB$_A$ ordering can be stable are examined here. The main geometric features of this structure are shown in Fig. 5. TGB$_A$ phase consists of slabs of length l_b exhibiting essentially bulk SmA ordering. These slabs are separated by grain boundaries (GB) of width $\sim \lambda$. Within each GB a lattice of screw dislocations resides; these dislocations are separated by a distance $l_d \sim l_b$ [3]. The presence of dislocations enables tilt between adjacent slabs giving rise to a global twisting of the LC structure along the $z-$axis of the coordinate frame. The volume of a representative TGB$_A$ unit cell, consisting of a SmA slab and a GB of surface l^2, is equal to $V_u \sim l_b l^2$. The length of each screw dislocation is estimated by l and their number within a GB is given by $N_{scr} \sim l/l_d$.
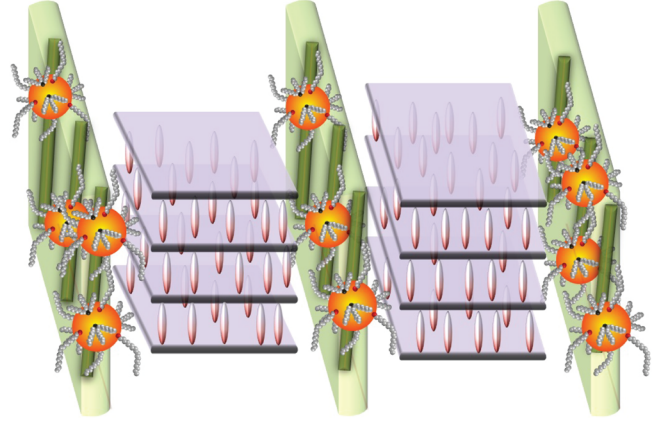

FIG. 5: A simple schematic illustration of the CdSSe NPs trapped in the screw dislocations is shown here.

V. ESTIMATED PHASE TRANSITION BEHAVIOR

In the following we describe the conditions under which even a minute concentration of dispersed NPs stabilizes the lattice of screw dislocations. The free energy costs of a phase within a unit cell V_u are labeled by $\Delta F^{(phase)}$. The corresponding average free energy density is given by $f^{(phase)} = \Delta F^{(phase)}/V_u$.

A. Pure samples

First, the case of pure LC (without NPs) is considered.
The ordering within N^* isdetermined by $\theta_\perp = q_{ch}z$, $\theta_\| = \pi/2$ and $\eta = 0$. The corresponding spatially-averaged free energy density $f^{(phase)} = \Delta F^{(phase)}/V_u$ equals

$$f^{(N^*)} = 0. \qquad (10)$$

Note that the saddle-splay elastic term can be mathematically transformed to the confining substrate. This contribution is neglected.

We describe the SmA ordering within a unit cell for $T < T_*$ by $\overrightarrow{n} = \overrightarrow{e}_x$ and $\psi = \eta_s e^{iq_0 x}$, yielding

$$f^{(SmA)} = -\frac{\alpha_0 |t|^2 \eta_0^2}{2} + \frac{Kq_{ch}^2}{2}. \qquad (11)$$

In the estimation of the free energy costs for the formation of TGB$_A$ structure it is assumed that an ideal SmA ordering is established within the smectic blocks. Across each GB of width $\sim \lambda$ the director field is approximately rotated by an angle [3]

$$\Delta\theta_\perp \sim \frac{d}{l_d} \sim \frac{d}{l_b}, \qquad (12)$$

and $\theta_{\parallel} = \pi/2$. The nematic elastic contribution reads

$$\int_0^{l_b} dz (\overrightarrow{n}.(\nabla \times \overrightarrow{n}) - q_{ch})^2 \sim \frac{\Delta\theta_{\perp}^2}{\lambda} - 2q_{ch}\Delta\theta_{\perp} + q_{ch}^2 l_b.$$

A global twisting of the LC configuration is enabled by GBs incorporating a lattice of parallel screw line dislocations. The core-size radius of each dislocation is approximated by ξ and within the cores the smectic ordering is essentially melted. The resulting average smectic condensation free energy within V_u is given by

$$F_c^{(TGB)} = -\frac{\alpha_0 |t|^2 \eta_0^2}{2}(V_u - V_{scr}). \quad (13)$$

Here $V_{scr} \sim N_{scr}l\pi\xi^2 \sim \pi l^2\xi^2/l_b$ is the volume occupied by the cores of screw dislocations. The other elastic contributions as well as the interactions among dislocations are not considered [33]. Note that this approximation works well only in the limit $l_d \gg \lambda$.

It follows

$$\begin{aligned} f^{(TGB)} &= \frac{K}{2}\left(\frac{\Delta\theta_{\perp}^2}{\lambda l_b} - \frac{2q_{ch}\Delta\theta_{\perp}}{l_b} + q_{ch}^2\right) \\ &\quad - \frac{\alpha_0 |t|^2 \eta_0^2}{2}(1 - \frac{\pi\xi^2}{l_b^2}). \end{aligned} \quad (14)$$

Our samples reveal that in the absence of NPs the phase exhibiting screw dislocations is absent, whereas it appears if even a minute amount of NPs is added. This suggests that in pure samples the triple point condition is roughly established. At the direct N^*-SmA phase transition (at $T = T_{NA}$) all the competing phases coexist, therefore $f^{(TGB)}(T_{NA}) = f^{(N^*)}(T_{NA}) = f^{(SmA)}(T_{NA})$. Consequently, $\lambda(T_{NA})\xi(T_{NA})q_0 q_{ch} = 1$ and

$$T_{NA} = T_*(1 - \lambda_0\xi_0 q_0 q_{ch}). \quad (15)$$

The critical value of the chirality wave vector enabling the triple point condition at $T = T_{NA}$ reads

$$q_{ch}^{(c)} \sim \frac{d}{\pi\xi^2}\left(1 - \sqrt{1 - \frac{\pi\xi^2}{\lambda l_b}}\right). \quad (16)$$

Therefore, the absence of chirality corresponds to an infinite value for l_b.

B. Samples with NPs

Next, it is assumed that NPs of an average volume concentration p are added (see Eq.(1)). It is assumed that NPs are predominantly assembled within the cores of dislocations. Consequently, they decrease the condensation free energy penalty which is required to introduce topological defects. Furthermore, due to their flexible tails the NPs disturb relatively weakly the local LC ordering. The corresponding main free energy penalties in the translational degree of order read

$$F_c^{(TGB)} = -\frac{\alpha_0 |t|^2 \eta_0^2}{2}(V_u - V_{scr} + N_{NP}v_{NP}). \quad (17)$$

However, the presence of NPs introduces boundaries where saddle-splay contributions might appear. Indeed, the director field variates along a radial direction from the center of a screw dislocation, yielding a finite saddle-splay contribution [32]. In the local cylindrical coordinate system attached to a screw dislocation defined by a unit vector triad $\{\overrightarrow{e}_\rho, \overrightarrow{e}_\varphi, \overrightarrow{e}_z\}$, where the center of cylindrically symmetric dislocation is placed at $\rho = 0$, the director field can be well parametrized by $\overrightarrow{n} \sim \cos\vartheta \overrightarrow{e}_z + \sin\vartheta \overrightarrow{e}_\varphi$. It holds $\overrightarrow{n}(\rho = 0) = \overrightarrow{e}_z$ and in the limit $\rho/d \gg 1$ the director distribution is well described by [32]

$$\vartheta = ArcTan(1/(\rho q_0)). \quad (18)$$

The corresponding saddle-splay contribution within V_u is estimated by $\Delta F_{24} = -N_{NP}\frac{K_{24}}{2}\int (\overrightarrow{n} \times \nabla \times \overrightarrow{n}).\overrightarrow{e}\,d^2\overrightarrow{r}$. The integration is carried out over a NP surface and $\overrightarrow{e}$ is the outer surface normal. Taking into account Eq.(18) we obtain

$$\frac{\Delta F_{24}}{V_u} \sim -\frac{Kpa_{24}}{2rd} \quad (19)$$

where r stands for the characteristic linear size of NP and $1/a_{24} \sim 4\pi^2(1 + 1/(4\pi r^2/d^2))^2(r/d)^3$. Note that this expression is approximate. Here the most important information is that the saddle-splay term yields a finite contribution if a NP is trapped within a screw dislocation. Therefore, in the presence of NPs it holds

$$f^{(TGB)}(p) \sim f^{(TGB)}(0) - p\left(\frac{\alpha_0 |t|^2 \eta_0^2}{2} + \frac{Ka_{24}}{2rd}\right), \quad (20)$$

while the impact of NPs on the other two phases is much smaller. Consequently, in the presence of NPs the stability range of TGB$_A$ phase is increased to a finite temperature interval that can be estimated by

$$\begin{aligned} \Delta T_{TGBA}(\chi) &\sim (T_* - T_{NA})p\left(1 + \frac{a_{24}}{q_{ch}^2 rd}\right)\frac{l_b^2}{\pi\xi^2} \sim \\ &\quad (T_* - T_{NA})\frac{\chi\rho_{LC}}{\rho_{NPs}}\left(1 + \frac{a_{24}}{q_{ch}^2 rd}\right)\frac{l_b^2}{\pi\xi^2} \end{aligned} \quad (21)$$

VI. CONCLUSIONS

This study has shown that the TGB_A and N_L^* phases can be induced by dispersing surface-functionalized CdSSe NPs, of a 3.5 nm diameter, in the liquid crystal CE8. Given the recent observation of NP-induced TGB_A and N_L^* phases in a different system of LC + NPs, it is suggested that this phenomenon exhibits a more general character. We anticipate that further research can unravel the precise role of NPs size and shape on inducing TGB order in chiral liquid crystals. Our recent preliminary results show that larger anisotropic NPs with similar surface treatment do not induce any TGB order in CE8.

VII. ACKNOWLEDGMENTS

[1] P. G. de Gennes, Solid State Commun. **10**, 753 (1972).

[2] S. R. Renn and T. C. Lubensky, Phys. Rev. A **38**, 2132 (1988).

[3] H. S. Kitzerow, *in The Physics of Liquid Crystals, Eds. H. S. Kitzerow and C. Bahr* (Springer, New York, 2001).

[4] J. W. Goodby, M. A. Waugh, S. M. Stein, E. Chin, R. Pindak, and J. S. Patel, Nature **337**, 449 (1989).

[5] H. T. Nguyen, A. Bouchta, L. Navailles, P. Barois, N. Isaert, R. J. Twieg, A. Maaroufi, and C. Destrade, J. Phys. II **2**, 1889 (1992).

[6] J. Fernsler, L. Hough, R. F. Shao, J. E. Maclennan, L. Navailles, M. Brunet, N. V. Madhusudana, O. Mondain-Monval, C. Boyer, J. Zasadzinski, et al., Proc. Natl. Acad. Sci. U.S.A. **102**, 14191 (2005).

[7] T. Chan, C. W. Garland, and H. T. Nguyen, Phys. Rev. E **52**, 5000 (1995).

[8] L. Navailles, P. Barois, and H. T. Nguyen, Phys. Rev. Lett. **71**, 545 (1993).

[9] L. Navailles, B. Pansu, L. Gorre-Talini, and H. T. Nguyen, Phys. Rev. Lett. **81**, 4168 (1998).

[10] V. Domenici, C. A. Veracini, V. Novotná, and R. Y. Dong, Chem. Phys. Chem. **9**, 556 (2008).

[11] T. Apih, V. Domenici, A. Gradišek, V. Hamplová, M. Kaspar, P. J. Sebastião, and M. Vilfan, J. Phys. Chem. B **114**, 11993 (2010).

[12] I. Dierking and S. T. Lagerwall, Liq. Cryst. **26**, 83 (1999).

[13] D. R. Nelson and H. S. Seung, Phys. Rev. B **39**, 9153 (1989).

[14] T. Bellini, L. Radzihovsky, J. Toner, and N. A. Clark, Science **294**, 1074 (2001).

[15] M. Marinelli, A. K. Ghosh, and F. Mercuri, Phys. Rev. E **63**, 061713 (2001).

[16] P. S. Clegg, C. Stock, R. J. Birgeneau, C. W. Garland, A. Roshi, and G. S. Iannacchione, Phys. Rev. E **67**, 021703 (2003).

[17] G. Cordoyiannis, G. Nounesis, V. Bobnar, S. Kralj, and Z. Kutnjak, Phys. Rev. Lett. **94**, 027801 (2005).

[18] G. Cordoyiannis, L. K. Kurihara, L. J. Martínez-Miranda, C. Glorieux, and J. Thoen, Phys. Rev. E. **79**, 011702 (2009).

[19] S. Relaix, R. L. Leheny, L. Reven, and M. Sutton, Phys. Rev. E **84**, 061705 (2011).

[20] Y. Reznikov, O. Buchnev, O. Tereshchenko, V. Reshetnyak, and A. Glushchenko, Appl. Phys. Lett. **82**, 1917 (2003).

[21] J. P. F. Lagerwall and G. Scalia, J. Mater. Chem. **18**, 2890 (2008).

[22] R. Basu and G. S. Iannacchione, Phys. Rev. E **81**, 051705 (2010).

[23] H. Yoshida, Y. Tanaka, K. Kawamoto, H. Kubo, T. Tsuda, A. Fujii, S. Kuwabata, H. Kikuchi, and M. Ozaki, Appl. Phys. Express **2**, 121501 (2009).

[24] E. Karatairi, B. Rožič, Z. Kutnjak, V. Tzitzios, G. Nounesis, G. Cordoyiannis, J. Thoen, C. Glorieux, and S. Kralj, Phys. Rev. E **81**, 041703 (2010).

[25] I. Dierking, W. Blenkhorn, E. Credland, W. Drake, R. Kociuruba, B. Kayser, and T. Michael, Soft. Matt. **8**, 4355 (2012).

[26] G. Cordoyiannis, P. Losada-Pérez, C. S. P. Tripathi, B. Rožič, U. Tkalec, V. Tzitzios, E. Karatairi, G. Nounesis, Z. Kutnjak, I. Muševič, et al., Liq. Cryst. **37**, 1419 (2010).

[27] G. Cordoyiannis, V. S. R. Jampani, S. Dhara, S. Kralj, V. Tzitzios, G. Basina, G. Nounesis, Z. Kutnjak, C. S. P. Tripathi, P. Losada-Pérez, et al., Soft Matt. **9**, 3956 (2013).

[28] M. Lavrič, G. Cordoyiannis, S. Kralj, V. Tzitzios, G. Nounesis, and Z. Kutnjak, Appl. Opt. **22**, E47 (2013).

[29] H. Haga and C. W. Garland, Phys. Rev. E **56**, 3044 (1997).

[30] H. Yao, K. Ema, and C. W. Garland, Rev. Sci. Instrum. **69**, 172 (1998).

[31] M. Kléman and O. D. Lavrentovich, *Soft Matter Physics* (Springer-Verlag, Berlin, 2003).

[32] S. Kralj and T. J. Sluckin, Phys. Rev. E **48**, R3244 (1993).

[33] I. Lelidis, C. Blanc, and M. Kléman, Phys. Rev. E **74**, 051710 (2006).